2011 American Control Conference
on O'Farrell Street, San Francisco, CA, USA
June 29 - July 01, 2011

Hybrid Powertrain Control with a Rapid Prototyping Research Platform

Yu Wang, Xingyong Song, Zongxuan Sun

Abstract—**As one of the most promising approaches for reducing automotive fuel consumption, hybrid powertrain has inspired extensive research efforts on system control and energy optimization. However, the time and cost of constructing or modifying a physical hybrid powertrain seriously affects the experimental investigation of the complicated system dynamics, so as to limit the development of the precise hybrid powertrain control and optimization. To provide an accurate and flexible hybrid powertrain emulation tool for developing the hybrid control methodologies, a rapid prototyping hybrid powertrain research platform, which employs a transient hydrostatic dynamometer to emulate the dynamics of various hybrid power sources and different hybrid architectures, is constructed. In this research platform, a three-level closed-loop control system is designed for realizing the hybrid powertrain emulation. With respect to the high/middle/low level systems, a suite of hybrid powertrain controllers including an adaptive driver model, an energy optimization strategy, a virtual hybrid torque controller and a dynamometer torque controller are designed and, further, their interactions are analyzed. Experimental results demonstrate that the proposed control system can achieve the precise emulation of the typical hybrid powertrain operation.**

I. Introduction

Powertrain hybridization, as an effective technical innovation with significant contributions on improving automotive fuel efficiency and reducing emissions, has drawn strong research interests from both the automotive industry and the academic community [1-7]. In recent years, extensive investigations on hybrid powertrain control have been conducted and various strategies have been proposed, including the rule-based control [2], the equivalent consumption minimization [1-4], the (stochastic) dynamic programming optimization [2-6] and the model predictive control [7], and so on. However, two technical barriers seriously limit our ability of accurately testing and continuously improving these control strategies or developing new control methods. First, the transient and interconnected dynamics within the hybrid powertrain system have significant impacts on the fuel efficiency, emissions and driving performance; also, they usually cannot be captured with low order mathematical models, which in turn demands the comprehensive experimental tests to validate and further, refine the proposed model-based control and optimization strategies. Second, the complex and time- consuming process of constructing a new hybrid system or changing the physical parameters of an existing hybrid system seriously slow down these experimental investigations.

To greatly expedite the investigation of hybrid powertrain control, a rapid prototyping hybrid powertrain research platform based on a transient hydrostatic dynamometer [8-9] is proposed. On the one hand, the combustion and emission behavior of the engine is too complicated to be modeled with a low-order approximation; on the other hand, the dynamics of the alternative power sources, hybrid transmission, driveline and vehicle load can be described with well-developed models. Thus, this research platform employs a high-bandwidth hydrostatic dynamometer to emulate the dynamic behaviors of the hybrid power sources (e.g., electric motor/generator) and vehicle loads, and interact with a multi-cylinder IC engine. The engine fuel efficiency and emissions can be measured and hence, the associated benefits and limitations of various hybrid powertrain architectures and control methodologies can be precisely quantified and systematically investigated by experiments, even without building a physical hybrid system.

Hardware-in-the-loop (HIL) testing has long been used in the study of the traditional and advanced powertrain dynamics. Recently, some systematic research efforts on the engine-in-the-loop testing for a parallel hybrid powertrain using an AC electric dynamometer have been reported [5], for evaluating hybrid propulsion concepts and transient emissions. In this paper, with a hydrostatic dynamometer as the torque tool, the work is targeted at experimentally investigating the torque-control based hybrid powertrain operation, for a power-split hybrid vehicle. However, to realize the hybrid powertrain dynamics emulation is very challenging. It combines a series of complex dynamic systems (engine, dynamometer, simulated alternative power sources and hybrid transmission) which brings in great difficulty to realize the precise control, especially for the engine (loading) torque control. Also, the two degree of freedom of a power-split hybrid system further increases the complexity of the powertrain control.

In order to overcome the above technical challenges on the proposed research platform, a three-level hybrid powertrain control and simulation system is built. At first, an adaptive driver model is designed to generate the power demand corresponding to the desired vehicle speed. Then, three-level control subsystems are designed, including a high-level controller for hybrid powertrain energy management, a middle-level controller for engine torque control, hybrid (electric) torque control and hybrid transmission/driveline HIL simulation, and a low-level controller for dynamometer torque control. The experimental results show that this hybrid powertrain rapid prototyping and control system is capable of emulating the dynamics of the hybrid vehicles.

Yu Wang (Email: wang0930@umn.edu), Xingyong Song (Email: songx122@umn.edu), and Zongxuan Sun (corresponding author, phone: 612-625-2107; Email: zsun@umn.edu) are with the Department of Mechanical Engineering, University of Minnesota, Twin Cities, MN 55455.

II. ARCHITECTURE DESIGN

The hybrid powertrain rapid prototyping and research platform is shown in Fig. 1, where the physical systems (engine and dynamometer) are highlighted in red, while the control and simulation components are in black.

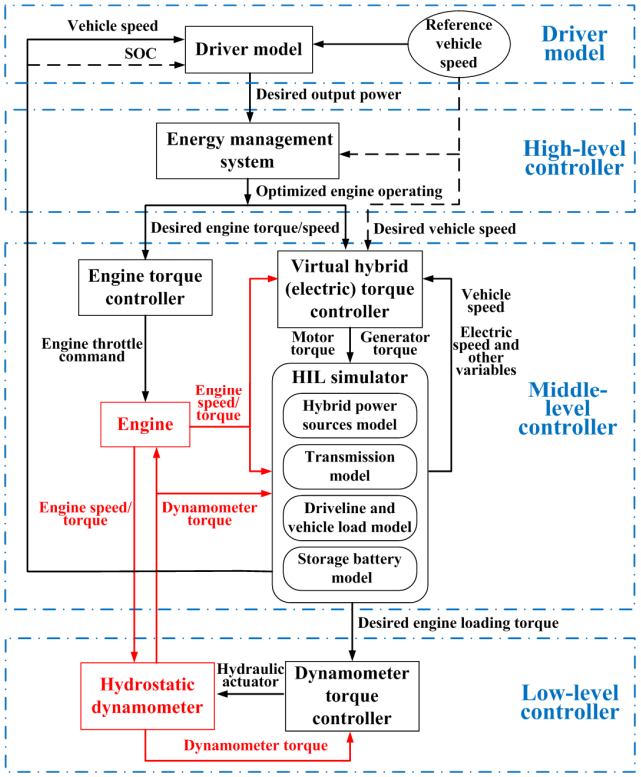

Fig. 1 Control system with the rapid prototyping hybrid powertrain research platform

The overall control and simulation system is built as a three-level closed-loop architecture:

Given a desired vehicle speed, the driver model produces a corresponding powertrain output power and then, in the high level system, for the desired power, the energy management system optimizes the engine operating profile to minimize the fuel consumption and emission; in the middle level system, the virtual hybrid (electric) torque controllers control the engine torque and virtual hybrid torques to realize the optimized engine operating profile and meanwhile, the HIL simulator is simulating the virtual hybrid powertrain system to produce the corresponding dynamic responses (primarily, the engine loading torque); in the low level system, the dynamometer is controlled to emulate the desired engine loading torque, so as to drive the engine to operate along the optimized profile. Consequently, measurement of the fuel consumptions and emissions will give an accurate performance evaluation of the current hybrid architecture or energy management strategy.

III. SYSTEM MODELING

A. *Power-split hybrid powertrain system modeling*

To ensure the HIL simulation can be viewed as a good substitute of the real dynamics, precise dynamic modeling for the hybrid powertrain systems is crucial. Here, the Toyota THS system [10-11], is used as a typical power-split electric hybrid configuration, as shown in Fig. 2. The dynamic models for the power-split transmission and driveline have already been investigated [3-7] and also presented in details in [8]:

$$J_{ec}\dot{\omega}_e = T_e - T_c$$

$$J_{gs}\dot{\omega}_g = T_s - T_g$$

$$\left(K_{ratio}J_{mr} + \frac{J_v}{K_{ratio}}\right)\dot{\omega}_v = T_r + T_m - \frac{T_v}{K_{ratio}}$$

$$\dot{SOC} = -\frac{V_{batt}}{2Q_{batt}R_{batt}} + \frac{\sqrt{V_{batt}{}^2 - 4\left[-T_g\omega_g\eta_g{}^{k1} + T_m\omega_m\eta_m{}^{k2}\right]R_{batt}}}{2Q_{batt}R_{batt}} \tag{1}$$

where,

$$\omega_m = \omega_v K_{ratio}$$

$$\omega_g S + \omega_m R = \omega_e (R+S)$$

$$T_v = \left[f_{tire}\cos(\phi_r) + \sin(\phi_r)\right]M_v g R_{tire} + 0.5\rho_a C_{drag} A_f \omega_v{}^2 R_{tire}{}^3$$

T_e, T_m, T_g, T_v, T_c, T_s and T_r are the engine torque, motor torque, generator toque, vehicle load torque, carrier gear torque, sun gear torque and ring gear torque, respectively. ω_e, ω_v, ω_m, and ω_g are the engine speed, vehicle speed, motor speed and generator speed, respectively. J_{ec}, J_{gs} and J_{mr} are the coupled moments of inertia of engine plus carrier gear, generator plus sun gear, and motor plus ring gear, respectively. J_v is the vehicle inertia. R and S are the radii of the ring gear and sun gear. K_{ratio} is the gear ratio between the electric motor and the driveline shaft. Q_{batt}, R_{batt} and V_{batt} are the rated capacity, internal resistance and voltage of the storage battery, respectively. Other parameters in Eq.(1) are explained in [8].

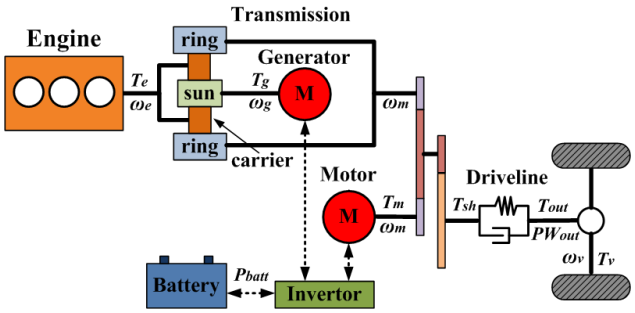

Fig. 2 Architecture of the power-split powertrain system

As the alternative power source in the hybrid electric vehicle, the dynamics of the PM (permanent magnet) AC synchronous machine are given as follows [12]:

$$L_d\dot{I}_d = U_d - R_s I_d + n_p L_q \omega_m I$$

$$L_q\dot{I}_q = U_q - R_s I_q - n_p L_d \omega_m I_d - \psi_m n_p \omega_m \tag{2}$$

$$T_m = \frac{3}{2}n_p\left[\psi_m I_q + \left(L_d - L_q\right)I_d I_q\right]$$

where the direct and quadrature axis voltages U_d, U_q, the direct and quadrature axis currents I_d, I_q, and the direct and quadrature axis inductances L_d, L_q are all measureable. R_s is the series phase resistance, n_p is the numbers of pole pairs, and Ψ_m is the permanent magnetic flux.

B. Hydrostatic dynamometer system modeling

The hydrostatic dynamometer consists of a main hydraulic loop (engine loading/motoring loop) and a bypass hydraulic loop (load sensing feedback loop). A ninth-order dynamic model for the whole dynamometer system has been built in [9]. Here only the dynamics of the engine loading/ motoring loop, which are directly involved with dynamometer torque/speed control, are given by:

$$\left(J_e + J_d\right)\dot{\omega}_e = T_e - T_d$$

$$\frac{V_{t2}}{\beta_e}\dot{P}_{out} = \frac{D_M}{2\pi}\omega_e + C_{im}\left(P_{in} - P_{out}\right) - C_{em}P_{out} - C_d A_{HS} w_{HS}\sqrt{\frac{2}{\rho}P_{out}} \tag{3}$$

where, $T_d = \frac{D_M}{2\pi}\left(P_{out} - P_{in}\right) + \frac{D_M}{2\pi}C_{da}\mu\omega_e + \frac{D_M}{2\pi}C_f\left(P_{in} + P_{out}\right)$

ω_e is the engine speed, P_{in} and P_{out} are the inlet and outlet pressure of the engine loading pump motor. T_e and T_d are the engine brake torque and dynamometer torque. J_e and J_d are the engine and dynamometer inertia. The control input for the hydraulic system, w_{HS} is the opening ratio of the control valve. The other parameters in Eq.(3) are explained in [8-9].

IV. CONTROL DESIGN

Targeted at emulating the real-world hybrid powertrain operation, the control system is designed to generate and experimentally realize the optimal engine operating profile at various hybrid operation modes, under realistic driving scenarios.

A. Adaptive driver model design

In virtual driving scenarios, a driver model is needed to transfer the driver's desired vehicle speed to the desired powertrain output power described by the commands on the accelerator/brake pedal. An ideal driver model should not only mimic the real-life mechanism of the human behavior, but also be capable of precisely tracking the speed reference as an experienced driver. Some PID based driver models have been conducted in [4-5]. To improve the tracking accuracy without loss of the similarity to the human behavior, an adaptive driver model is built.

From Eq. (1), the vehicle driveline dynamics is given by:

$$J_v\dot{\omega}_v = \frac{PW_{out}}{\omega_v} - f_{tire}M_v gR_{tire} - 0.5\rho_a C_{drag}A_f\omega_v^2 R_{tire}^3 \tag{4}$$

where PW_{out} is the desired powertrain output power. Here we assume the road grade $\phi_r = 0$.

Further, Eq. (4) can be transformed to the error dynamics with the speed error $e_v = \omega_{v\_des} - \omega_v$, given by:

$$J_v\dot{e}_v = -\frac{PW_{out}}{\omega_v} + \sigma_1\dot{\omega}_{v\_des} + \sigma_2 + \sigma_3\omega_v^2 \tag{5}$$

where, $\sigma_1 = J_v$, $\sigma_2 = f_{tire}M_v gR_{tire}$, $\sigma_3 = 0.5\rho_a C_{drag}A_f R_{tire}^3$

Since the variables e_v, ω_v and $\dot{\omega}_{v\_des}$ can be captured by the driver in real time, it is reasonable for the driver to command the pedals with a corresponding power output:

$$PW_{out} = K_1 e_v\omega_v + \hat{\sigma}_1\dot{\omega}_{v\_des}\omega_v + \hat{\sigma}_2\omega_v + \hat{\sigma}_3\omega_v^3 \tag{6}$$

where, $\hat{\sigma}_1$, $\hat{\sigma}_2$ and $\hat{\sigma}_3$ are the driver's estimates for σ_1, σ_2 and σ_3. K_1 is a positive gain.

Substituting Eq. (6) into Eq. (5) yields:

$$J_v\dot{e}_v = -K_1 e_v + \tilde{\sigma}_1\dot{\omega}_{v\_des} + \tilde{\sigma}_2 + \tilde{\sigma}_3\omega_v^2 \tag{7}$$

where, $\tilde{\sigma}_1 = \sigma_1 - \hat{\sigma}_1$, $\tilde{\sigma}_2 = \sigma_2 - \hat{\sigma}_2$, $\tilde{\sigma}_3 = \sigma_3 - \hat{\sigma}_3$.

To enable the stability of the error dynamics, an adaptive parameter tuning dynamics is utilized. For the nonlinear system in Eq. (7), a Lyapunov function is given by:

$$V\left(e_v, \sigma\right) = \frac{1}{2}J_v e_v^2 + \frac{1}{2}K_2\tilde{\sigma}_1^2 + \frac{1}{2}K_3\tilde{\sigma}_2^2 + \frac{1}{2}K_4\tilde{\sigma}_3^2 \tag{8}$$

where K_2, K_3 and K_4 are all positive gains.

With the adaptive parameter error dynamics,

$$\dot{\hat{\sigma}}_1 = -\dot{\tilde{\sigma}}_1 = \frac{\dot{\omega}_{v\_des}e_v}{K_2},\quad \dot{\hat{\sigma}}_2 = -\dot{\tilde{\sigma}}_2 = \frac{e_v}{K_3},\quad \dot{\hat{\sigma}}_3 = -\dot{\tilde{\sigma}}_3 = \frac{\omega_v^2 e_v}{K_4} \tag{9}$$

the asymptotic stability of the nonlinear system in Eq. (7) is guaranteed due to the Barbalat's lemma [13]. Consequently, the speed error is eliminated by the adaptive driver dynamics.

B. High-level control: experiment-oriented DP (dynamic programming)-based energy optimization strategies

A typical global optimization tool, dynamic programming, which has been widely investigated in the hybrid powertrain control area [3-6], is utilized as the energy management strategy and specially designed for the experiments.

The cost function used in the DP based energy management strategy is designed to minimize the fuel consumption and keep the SOC sustained in a limited bound, given by:

$$J = \sum_{k=0}^{N-1}\left\{FC(k) + f_{\omega e}\left[\omega_e(k) - \omega_e(k-1)\right]^2 + f_{Te}\left[T_e(k) - T_e(k-1)\right]^2\right\} + f_{soc}\left[SOC(N) - SOC(N)_{des}\right]^2 - m_{soc}\left[SOC(N) - SOC(N)_{des}\right] \tag{10}$$

where FC is the fuel consumption in a single sampling step, $SOC(N)$ and $SOC(N)_{des}$ are the actual and desired battery SOC at the final step, f_{soc} is the SOC sustaining factor and m_{soc} is the SOC variation compensation factor. To avoid unnecessary engine torque and speed vibrations, the penalty factors $f_{\omega e}$ and f_{Te} are used to smooth the optimized operating trajectories.

C. Mid-level control: virtual hybrid torque control and electric machine control

In the mid-level system, the desired vehicle/engine operation ω_v (or PW_{out}), ω_e and T_e will be realized by controlling the engine throttle and virtual hybrid torques T_m and T_g. Further, to control T_m and T_g, the servo control for the electric machines should be achieved.

(1) Virtual hybrid torque control

The mid-level control objective is to simultaneously realize the desired ω_v, ω_e and T_e by means of the precise torque control of the hybrid power sources. In the high level control, the DP optimization has generated the optimized trajectories T_m and T_g, which theoretically can achieve the desired hybrid

powertrain operation. However, experimental results show that the pure open-loop control using the optimized inputs T_m and T_g cannot ensure the stability of the whole system. It can be attributed to the fact that the optimization is based on some simplified dynamic models without considering the complex engine dynamics. Thus, it is important to design the control of T_m and T_g to ensure both the system stability and precise tracking of the system variables (ω_v, ω_e and T_e, etc.).

The engine throttle is dedicated to control the engine torque T_e using a calibrated engine map. Consequently, the hybrid torque control is formulated into a two-inputs (T_m and T_g), two-outputs (ω_v and ω_e) problem. Here, a hybrid torque control is designed to transform it into two single-input, single-output controls: the generator is used as a speed compensator to track ω_e (indirectly, T_e), to realize the optimal engine operation; simultaneously, the motor is used as a power compensator to track PW_{out} (equivalently, ω_v), to realize the desired vehicle operation [3-4, 14-15].

The generator torque (engine speed) control is critical to realize the control target. First, for the planetary gear set, the transmission dynamics are given by:

$$J_{ec}\dot{\omega}_e = T_e - T_c,\quad J_{gs}\dot{\omega}_g = T_s - T_g,\quad T_s(R+S) = T_c S \qquad (11)$$

If the high-bandwidth generator inertia dynamics is neglected compared with the low-bandwidth engine inertia dynamics, the transmission dynamics can be simplified by:

$$J_{ec}\dot{\omega}_e = T_e - \frac{R+S}{S}T_g \qquad (12)$$

where the engine torque is a mapping of the engine speed and throttle opening, so that it cannot be directly controlled but measureable. A torque/speed feedback control is given by:

$$T_{g\_des} = \frac{S}{R+S}T_e - \frac{S}{R+S}J_{ec}\dot{\omega}_{e\_des} + K_p e_{\omega_e} + K_I\int e_{\omega_e}dt \qquad (13)$$

where, $e_{\omega e} = \omega_e - \omega_{e\_des}$, K_P and K_I are both positive gains.

Substituting Eq. (13) into Eq. (12) yields:

$$J_{ec}\dot{e}_{\omega_e} + \frac{R+S}{S}K_p e_{\omega_e} + \frac{R+S}{S}K_I\int e_{\omega_e}dt = dis(t) \qquad (14)$$

where, a disturbance *dis(t)* is introduced to represent the actual torque control errors which always exist in experiments. Or, in the *s*-domain (*s* is the Laplace operator), it is given by:

$$\frac{E_{\omega_e}(s)}{Dis(s)} = \frac{s}{J_{ec}s^2 + \frac{R+S}{S}K_p s + \frac{R+S}{S}K_I} \qquad (15)$$

It is obvious that this control law can eliminate the constant system disturbance or perturbation for engine speed control. Tuning of the gains K_P and K_I will produce a good pole placement for improving the system stability.

On this basis, with the derived T_{g_des} in Eq. (13) as a time-varying parameter, the motor torque T_m can be used to compensate the powertrain output power, given by:

$$T_{m\_des} = \frac{PW_{out\_des}}{\omega_m} - T_{g\_des}\frac{R}{S} \qquad (16)$$

(2) Virtual electric machine control

Given the desired T_{g_des} and T_{m_des}, the electric machine servo control will achieve the torque tracking by controlling the two-phase input voltages U_d and U_q.

Form the electric machine dynamics in Eq. (2), there is a nonlinear mapping among the torque T_m and the currents I_d and I_q. To simplify the torque control, I_d can be regulated to zero, so as to build a linear mapping between T_m and I_q, as:

$$I_{q\_des} = \frac{2T_{m\_des}}{3n_p\psi_m} \qquad (17)$$

Then, the current-voltage error dynamics are given by:

$$\begin{aligned} L_d\dot{e}_{I_d} &= -R_s e_{I_d} - n_p L_q\omega_m I_q - U_d \\ L_q\dot{e}_{I_q} &= -R_s e_{I_q} + L_q\dot{I}_{q\_des} + R_s I_{q\_des} + n_p L_d\omega_m I_d + \psi_m n_p\omega_m - U_q \end{aligned} \qquad (18)$$

where, the current errors $e_{I_d} = -I_d$, $e_{I_q} = I_{q\_des} - I_q$

The state-feedback control law for the two inputs is:

$$\begin{aligned} U_d &= -n_p L_q\omega_m I_q \\ U_q &= L_q\dot{I}_{q\_des} + R_s I_{q\_des} + n_p L_d\omega_m I_d + \psi_m n_p\omega_m \end{aligned} \qquad (19)$$

Substituting this control law into Eq. (18) yields a asymptotically stable system, which ensures the electric motor (or generator) torque track the desired trajectories generated by the hybrid torque controllers.

D. Low-level control: feedback-linearization based dynamometer torque control

With regards to the engine-dynamometer system, the low-level control target is to manipulate the dynamometer torque T_d by controlling the input w_{HS} to mimic the torque behavior of the virtual hybrid powertrain (i.e., track the HIL simulated engine loading torque). For the nonlinear dynamics in Eq. (3), a feedback linearization controller is designed.

First, a direct mapping between the dynamometer torque T_d and engine loading pump outlet pressure P_{out} exists as:

$$T_d = \frac{D_M}{2\pi}(1+C_f)P_{out} - \frac{D_M}{2\pi}(1-C_f)P_{in} + \frac{D_M}{2\pi}C_{da}\mu\omega_e \qquad (20)$$

It is equivalent to track the outlet pressure P_{out} instead of dynamometer torque T_d, if only P_{in} and ω_e are measureable. Thus, the pressure dynamics is given for pressure tracking:

$$\begin{aligned} \dot{P}_{out} &= \frac{D_M\beta_e}{2\pi V_{t2}}\omega_e - \frac{\beta_e}{V_{t2}}(C_{im}+C_{em})P_{out} + \frac{\beta_e}{V_{t2}}C_{im}P_{in} \\ &\quad - \frac{\beta_e}{V_{t2}}C_d A_{HS}\sqrt{\frac{2}{\rho}P_{out}}\,w_{HS} \\ &= a(\omega_e, P_{out}, P_{in}, D_M) + b(P_{out})w_{HS} \end{aligned} \qquad (21)$$

where $a(\omega_e, P_{out}, P_{in}, D_M)$ and $b(P_{out})$ are both functions of the state variables and measurable time-varying parameters.

With respect to Eq. (21), a feedback linearization control law which asymptotically stabilizes the system is designed by:

$$w_{HS} = \left(-\lambda_1 e_{P_{out}} - \lambda_2\int e_{P_{out}}dt - a + \dot{P}_{out\_des}\right)\Big/ b \qquad (22)$$

where $e_{Pout} = P_{out} - P_{out\_des}$, λ_1 and λ_2 are positive feedback gains. The integral term is added to reduce the tracking error

due to some unmodeled dynamics. The pressure P_{out_des} is derived via Eq. (20) with the pre-calculated torque T_{d_des}. A nonlinear model-based inversion control can also be applied [9] to achieve precise torque tracking.

With the accurate low-level control, the transient hybrid torque (or, pressure) emulation can be realized in experiments. In Fig. 3, it is shown that the system is capable of precise tracking of the desired pressure/torque profiles.

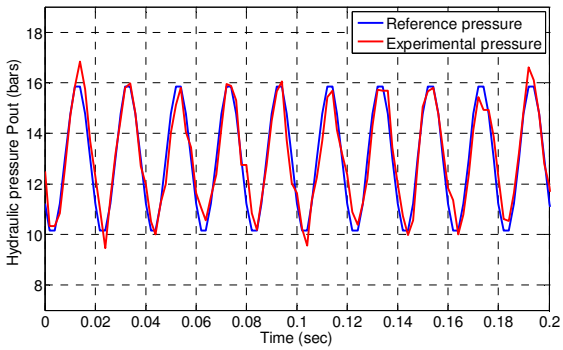

Fig. 3 The outlet pressure tracking in the low-level system

E. Dynamic analysis of the closed-loop system

The overall three-level systems consist of three control loops: the inner loop (engine loading torque control loop), the outer loop (virtual hybrid powertrain control loop) and the upper loop (the energy management control loop) as shown in Fig.4. In this paper, the DP energy management strategy is running offline, so that the influence of the upper loop for the system dynamics can be temporarily neglected.

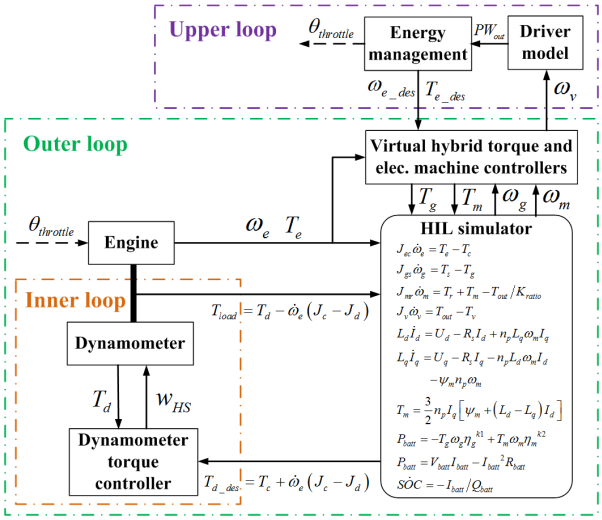

Fig. 4 The closed-loop control system

The dynamic interactions between the inner and outer control are realized via the HIL simulation: in the outer loop, the desired ω_v and ω_e in the virtual "engine - hybrid powertrain" system are controlled by virtual hybrid torque controllers. Within the HIL simulation, the virtual engine loading torque (i.e., the torque on the carrier gear) T_c, is produced as the torque reference for the inner control loop; in the inner loop, the dynamometer torque T_d is controlled to track the torque reference in the engine-dynamometer system and then, the real-world engine torque T_e and engine loading torque T_d in the inner loop are fed back to the HIL simulator.

Correspondingly, the control logic is summarized by: in the inner loop, the control system controls the engine loading torque to track the reference and on this basis, in the outer loop, the optimized engine and vehicle speed are simultaneously realized by means of adjusting the reference of the engine loading torque. With the control for both the engine speed and engine throttle, the optimized engine torque will be realized. Thus, the precise engine loading torque control is crucial to the whole inner-outer loop control. With this target, however, some challenges do exist: the tracking error of the engine loading torque e_{Td} can be treated as the torque disturbance *dis(t)* defined in Eq. (14), so that Eq.(15) essentially shows the dynamic relationship between the engine speed control and engine loading torque control. In transients, the torque tracking error from the inner loop could excite the speed tracking error in the outer loop. Subsequently, the speed error will be fed back to the engine speed control (mid-level control) in the outer loop and then the torque control (low-level control) in the inner loop, so as to further degrade the torque tracking. To fully address this complicated dynamic problem, an H_∞ robust control for mid-level is being investigated.

V. EXPERIMENTS RESULTS

To demonstrate the capability of the hybrid powertrain control system with the research platform, extensive experiments have been conducted. As an example, part of the Highway Fuel Economy Test (HWFET) driving circle is chosen and slightly modified as the desired vehicle speed.

Figures 5-7 show the experimental trajectories of all the key variables that concern the vehicle, engine and virtual hybrid power sources. In Fig. 5, the experimental results (vehicle speed, engine speed, engine loading torque and generator/ motor speeds) precisely track the desired trajectories. Especially for the engine loading (dynamometer) torque, the accurate tracking demonstrates the performance of the torque-control based hybrid powertrain control system. Fig. 6-7 show the experimental generator/motor torques vs. the optimized generator/motor torques. As discussed before, open loop control with the optimized electric torques triggers the system instability. Thus, the feedback control for the electric torques is designed, which shows some differences from the optimized ones. As a result, the experimental SOC of the battery in Fig.5 is also different from the optimized trajectory.

VI. CONCLUSION

This paper presents the design and experimental investigation of the hybrid powertrain control system with a rapid prototyping hybrid powertrain research platform. With a high-bandwidth hydrostatic dynamometer as torque mimicking tool and accurate hybrid transmission system models as mimicking target, the research platform can emulate the dynamic behaviors of any kinds of hybrid power sources and hybrid architectures. With an adaptive driver model, a

three-level closed-loop control system which combines a DP based energy management strategy, a feedback hybrid torque (electric machine) control and a feedback linearization based dynamometer torque control, is designed. The experimental results demonstrate the capability of the hybrid powertrain research platform.

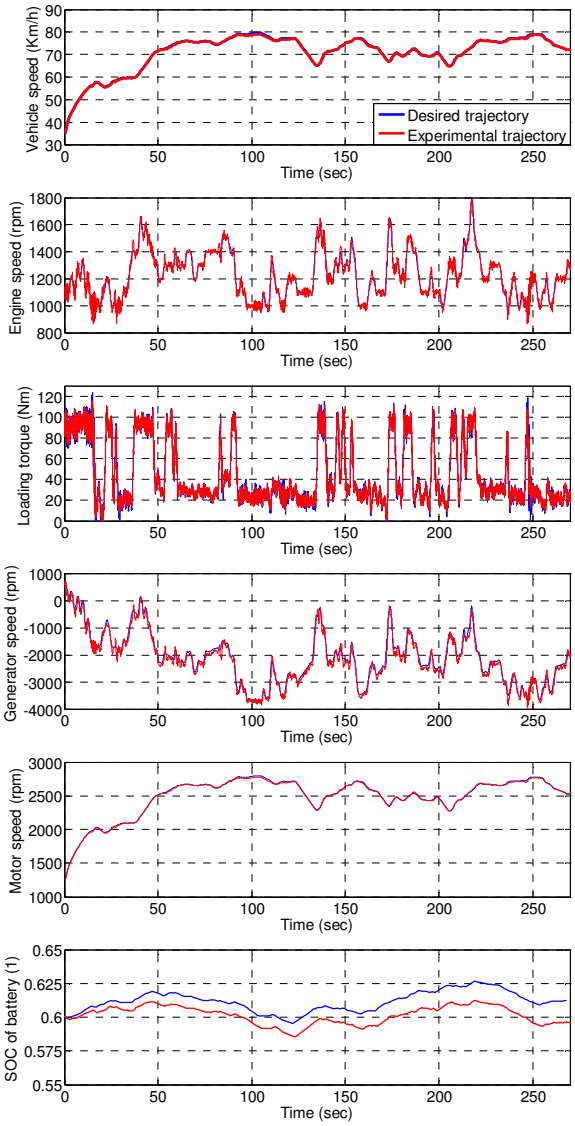

Fig. 5 Tracking trajectories of the main variables in the hybrid powertrain

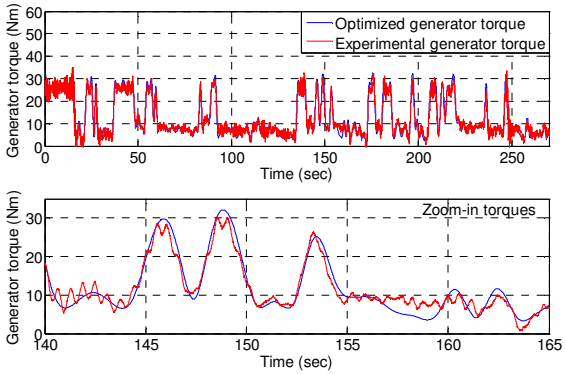

Fig. 6 The optimized and actual generator torque trajectories

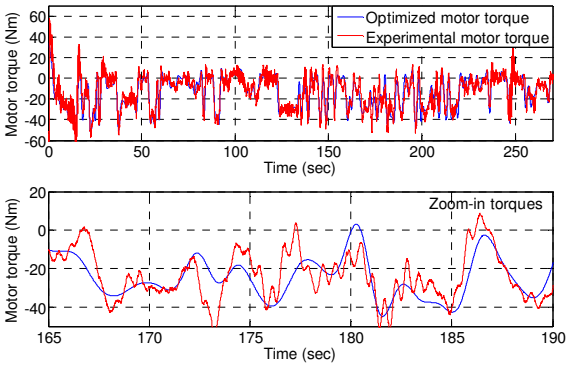

Fig. 7 The optimized and actual motor torque trajectories

VII. AVKNOWLEDGEMENTS

The authors would like to gratefully acknowledge the NSF support under the grant number CMMI-0959741.

REFERENCES

[1] Sciarretta, A., Guzzella, L. “Control of hybrid electric vehicles”, IEEE Control Systems Magazine, Vol. 27, No. 2, 2007: pp. 60–70.

[2] Pisu, P., Rizzoni, G. “A comparative study of supervisory control strategies for hybrid electric vehicles”, IEEE Transactions on Control Systems Technology, Vol.15, No.3, 2007: pp. 506-518.

[3] Liu, J., Peng, H., “Modeling and control of a power-split hybrid vehicle”, IEEE transactions on control systems technology, Vol. 16, No.6, 2008: pp1242-1251.

[4] Liu, J., “Modeling, configuration and control optimization of power-split hybrid vehicles”, Ph.D. dissertation, University of Michigan, 2007.

[5] Filipi, Z., Fathy, H., Hagena J., et al, “Engine-in-the-Loop testing for evaluating hybrid propulsion concepts and transient emissions – HMMWV case study”, SAE technical paper, Detroit, Michigan, 2006-01-0443.

[6] Tate, E., Grizzle, J., Peng, H., “SP-SDP for fuel consumption and tailpipe emissions minimization in an EVT hybrid”, IEEE Transactions on Control Systems Technology, Vol.18, No.3, 2010: pp. 673-687.

[7] Borhan, H., Vahidi, A., Phillips, A., et al, “Predictive energy management of a power-split hybrid electric vehicle”, Proceedings of the American Control Conference, Saint Luis, Missouri, 2009: pp. 3970-3976.

[8] Wang, Y., Sun, Z., “A hydrostatic dynamometer based hybrid powertrain research platform”, Proceedings of the International Symposium on Flexible Automation, UPS-2739, Tokyo, Japan, 2010.

[9] Wang, Y., Sun, Z., Stelson, K. A., “Modeling, control and experimental validation of a transient hydrostatic dynamometer”, IEEE Transactions on Control Systems Technology, DOI 10.1109/TCST.2010.2082542.

[10] Duoba, M., Ng, H., Larsen, R., “Characterization and compassion of two hybrid electric vehicles (HEVs) – Honda Insight and Toyota Prius”, SAE technical paper, Detroit, Michigan, 2001-01-1335.

[11] Meisel, J., “An analytical foundation for the Toyota Prius THS-II powertrain with a comparison to a strong parallel hybrid-electric powertrain”, SAE technical paper, Detroit, Michigan, 2006-01-0666.

[12] Chen, X., Shen, S., “Comparison of two permanent-magnet machines for a mild hybrid electric vehicle application”, SAE technical paper, Detroit, Michigan, 2008-01-1552.

[13] Khalil, H. 2002. Nonlinear systems. Prentice Hall, pp. 322-329.

[14] Kimura, A., Abe, T., Sasaki, S., “Drive force control of a parallel-series hybrid system”, J.SAE Review, Vol.20, 1999, pp337-341.

[15] Ai, X., Anderson, S., “An electro-mechanical infinitely variable transmission for hybrid electric vehicles”, SAE technical paper, Detroit, Michigan, 2005-01-0281.